Antenna Tracking System for Robust Communication in Ingestible Electronics

Ziyao Zhou*, Chenyang Ren*, Boyan Li*, Chen Shen*, Rong Tan*, Hen-Wei Huang*†
Email: {ZHOU0557, CHENYANG002, BOYAN001}@e.ntu.edu.sg, {shenchen, rong.tan, henwei.huang}@ntu.edu.sg
*School of Electrical and Electronic Engineering, Nanyang Technological University, Singapore
†LKC School of Medicine, Nanyang Technological University, Singapore

***Abstract*—Antenna tracking is common yet critical for maintaining robust communication. However, tracking ingestible electronics (IE) is laborious and tedious, as their orientation becomes entirely unpredictable after ingestion. The conventional solution is to maximize transmission power (TXP) to compensate for misalignment, which significantly increases power consumption. Another way is to randomly change the orientation of the receiver (RX), which increases uncertainty. In this study, we propose an orientation-aware system that embeds inertial measurement units in both the IE and RX to estimate real-time orientation and dynamically align the RX antenna. Attitude estimation is performed using the Mahony filter, and quaternion-based motion was visualized in Blender. We evaluated four antenna types—Chip, Helical, PCB, and FPC—and found that each exhibited pronounced directionality, with received signal strength indicator (RSSI) standard deviations of at least 5 dB. Continuous beam tracking based on real-time orientation yielded an average gain of 4 dB, allowing for a 4 dB reduction in TXP and a corresponding 32% decrease in peak current draw. Even under complex motion, the RX maintained near-optimal RSSI (–40 dBm) with minimal fluctuation. These results demonstrate that our system enhances communication stability, reduces power consumption, and enables precise, dynamic tracking of ingestible electronics.**

***Index Terms*—Ingestible Electronics, Antenna, Directivity, IMU, Attitude Estimation, Quaternions**

I. Introduction

The advancement of ingestible electronics (IE) has enabled real-time, in situ monitoring of the gastrointestinal (GI) tract [1]–[3]. However, wireless communication remains a significant challenge due to strong electromagnetic wave attenuation caused by tissue absorption [4]–[6]. Additionally, the random and uncontrollable orientation of IE within the GI tract further degrades communication quality, as it prevents effective alignment between the IE antenna and the external receiver (RX), as shown in Figure 1. To address this, a variety of antenna designs have been developed to produce omnidirectional radiation patterns, aiming to support orientation-insensitive communication within the body [3], [7], [8].

To date, no antenna design achieves truly omnidirectional performance. As a result, maximum transmission power (TXP) is often employed to compensate for antenna misalignment, significantly reducing energy efficiency. Simultaneously, the RX must blindly adjust its position and orientation in search of the optimal signal direction, introducing additional uncertainty and instability in the communication link.

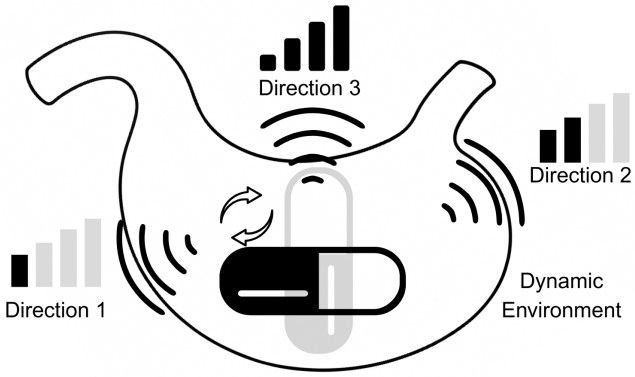

Fig. 1: The siganl strength of a wireless ingestible electronics differs from orientation, and the best beam changes. The maximum TXP is used, and the receiver's position is changed randomly to achieve stable communication.

In this work, we propose a dual-IMU system—one embedded in the IE and the other in the RX—to enable real-time attitude estimation and feedback-guided alignment for optimal signal reception. The RX, equipped with a high-gain directional antenna, dynamically orients itself toward the optimal beam direction as indicated by 3D visual feedback. This approach allows for reduced TXP while maintaining stable communication quality. The IMU-based feedback system guides the user in real time to align the RX for maximum signal strength with less uncertainty. This study investigates various attitude estimation algorithms, characterizes the radiation patterns of four commonly used antenna types, and demonstrates that visualized orientation feedback significantly improves signal quality and energy efficiency.

II. Methodology

A. Attitude Estimaition and Visualization

Attitude estimation enables the IE and RX to be represented simultaneously within the same coordinate system, yielding their relative positional relationship [9]. Visualization enables operators to see relative relationships and perform corresponding actions intuitively.

This work was supported by the Nanyang Professorship, the MOE Tier 1 grant RG71/24, and the MTC MedTech Programmatic Fund M24N9b0125. *(Ziyao Zhou and Chenyang Ren contributed equally to this work.)*

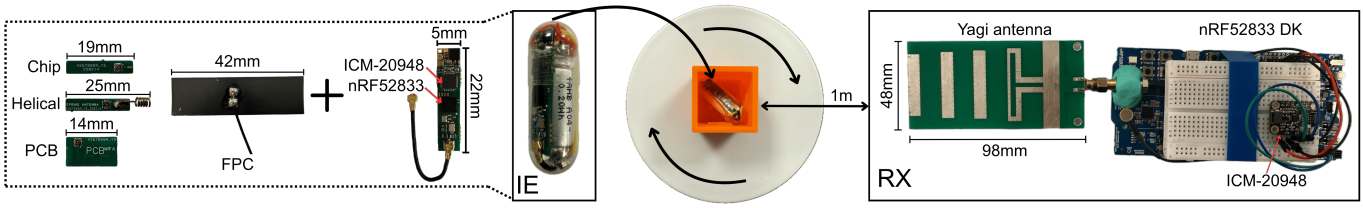

Fig. 2: Testing platform for antenna directivity. (a) Design of the IE main PCB and four supporting antennas; the complete IE will be assembled into a 000-size capsule. (b) Constant-speed rotation platform with a cubic container. This cube has three faces labeled. (c) The receiver is using a highly directional 2.4 GHz Yagi antenna.

We selected the Mahony filter for its high accuracy, comparable to that of the extended Kalman filter (EKF), and its superior performance over the Madgwick filter in dynamic scenarios involving moderate-to-rapid motion [10]. Moreover, it relies solely on quaternion-error proportional-integral updates and eschews matrix and gradient iterations, which significantly reduces computational complexity and accelerates convergence [11]. Its complementary design further attenuates high-frequency jitter and low-frequency drift without requiring explicit noise modeling [12].

The quaternions obtained after attitude estimation are used to rotate the corresponding models in Blender.

B. Antenna Directional Characteristics

We selected four different types of 2.4 GHz antenna, which are commonly used in ingestible electronics: Chip [13], Helical [14], PCB [15], and FPC [16], to characterize their directional patterns and identify whether each antenna has peak-beam orientation. The four antennas' PCB and the main PCB are shown in Figure 2(a).

The main PCB connects to each antenna via an IPEX connector and integrates an nRF52833 MCU with an ICM-20948 IMU. The MCU's TXP is set to 8 dBm. The RX platform uses an nRF52833 DK paired with the same IMU and a 2.4 GHz Yagi antenna, whose high directivity provides increased link gain and beam resolution [17].

The experiment was performed on a rooftop to minimize electromagnetic interference. The IE was mounted inside a cube at the center of the rotation platform (Figure 2(b)). First, the cube's X face contacted the platform and was rotated while the RX antenna, located 1 m away, recorded received signal strength indicator (RSSI) over a full 360° sweep. The same procedure was then repeated with the cube's Y and Z faces to capture RSSI variations along all three planes.

C. Antenna following

The antenna following procedure is as follows. First, with the IE held stationary, the operator adjusts the RX until the RSSI is maximized; during this step, the beam model remains rigidly attached to the RX. Second, once the optimal orientation is identified (maximum RSSI), the beam model is locked onto the IE, indicating the IE's best direction. Finally, if the IE rotates dynamically, the operator rotates the RX antenna to realign with the beam model, thereby maintaining the optimal link.

To validate this method, the previous test platform shown in Figure 2(b) was placed inside a black box. With the platform stationary, the RX antenna was positioned 1 m away and adjusted until RSSI was maximized; this orientation was then registered to the IE model. In the first trial, the RX was fixed at the current orientation while the IE completed a 360° rotation, and RSSI was recorded continuously. In the second trial, the RX antenna was continuously steered to follow the recorded optimal beam direction as the IE rotated, and RSSI was logged over a full rotation.

We measured the nRF52833's maximum current consumption across different TXP settings. Using the antenna following system may yield a gain that allows a corresponding reduction in current consumption while having equivalent communication performance.

To evaluate accuracy under noisy GI motion, the IE was placed inside a container, which was hung in midair with no obstructions around it. We identified the maximum and minimum RSSI at 1 m and locked the maximum beam orientation to the IE model. Then, we applied four random disturbances to the container. After each disturbance, once the IE had stabilized, the RX was realigned to the locked beam direction, and the resulting RSSI was recorded.

III. RESULTS AND DISCUSSION

A. Antenna Directional Characteristics

Figure 3 presents the antenna measurement results. Subplots (a)–(d) correspond to the Chip, Helical, PCB, and FPC antennas, respectively. In each subplot, the red, green, and blue curves show RSSI readings on the X, Y, and Z planes; each point's angle is measured from the initial position, and its radial distance represents the RSSI magnitude. All four plots display uneven surfaces, indicating that the radiated power is not uniformly distributed across planes. In other words, each antenna exhibits clear directionality.

Table I compares statistical results for four antennas, combining data from their X, Y, and Z planes. Each antenna's standard deviation exceeds 5 dB, confirming directionality. Based on average RSSI, the Helical antenna has the highest signal strength, the FPC antenna the lowest, and the Chip and PCB antennas exhibit similar performance at -49 dBm. Considering that the Chip has a smaller form factor and is easier to integrate in designs, and to validate the antenna-following

functionality under conditions closest to the "omnidirectional" limit, subsequent experiments will use the Chip antenna.

B. Antenna following

The static receiving result versus the actively tracking result is shown in Figure 4(a). The purple curve represents the RSSI readings when the IE completes one full rotation while the RX is fixed; the yellow curve represents the RSSI during active tracking of the optimal direction. It can be seen that the yellow curve approximates a circle of radius -45 dBm, whereas the purple curve is uneven.

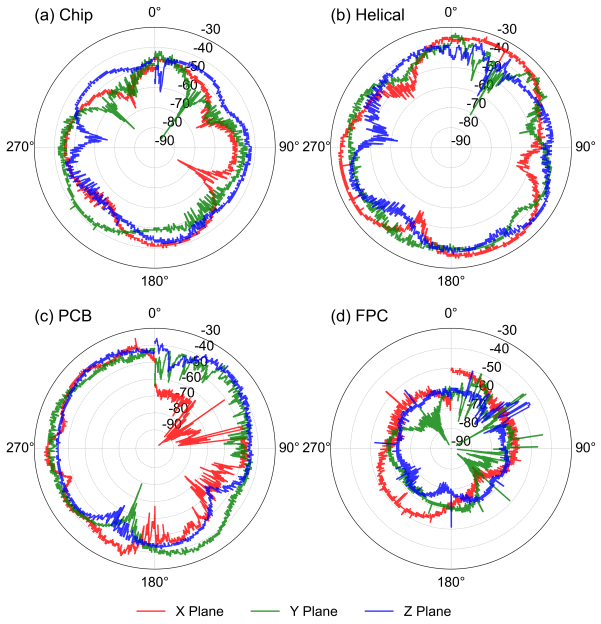

Fig. 3: Directional characteristics of four antennas. All antennas exhibit directionality in three directions.

TABLE I: Radiation characteristics of four antennas, showing RSSI maximum (dBm), minimum (dBm), average (AVG in dBm), and standard deviation (STD in dB).

Antenna	MAX	MIN	AVG	STD
Chip	−38	−85	−49	5
Helical	−32	−71	−41	5
PCB	−35	−98	−49	11
FPC	−44	−88	−63	6

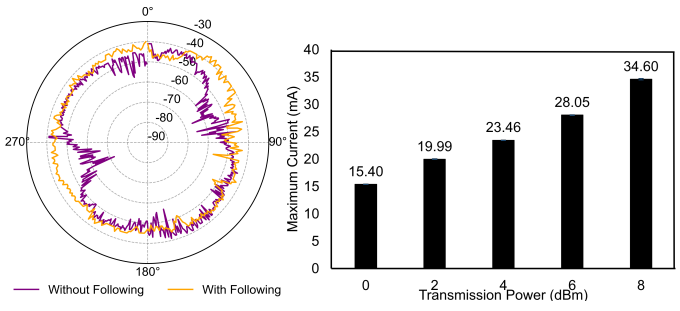

Fig. 4: (a) RSSI comparison with and without antenna following. (b) Maximum current under different TXP for nRF52833.

Table II provides a statistical comparison of the static and active-tracking RSSI curves. Although their maximum RSSI values are similar, the minimum differs by 15 dB. Over a full 360° rotation, active tracking raises the average RSSI from –48 dBm to –44 dBm (a 4 dB gain) and reduces the standard deviation from 5 dB to 3 dB, thereby stabilizing the signal.

TABLE II: RSSI statistics with and without following, showing RSSI maximum, minimum, average, and standard deviation.

Scenario	MAX	MIN	AVG	STD
Without following	−41	−72	−48	5
With following	−39	−57	−44	3

Based on the system's current consumption shown in Figure 4(b), assuming a 4 dB gain has been obtained, we can avoid driving the IE at its maximum TXP (8 dBm for the nRF52833) and instead set TXP = 4 dBm. In doing so, maximum current consumption drops 32% from 34.6 to 23.46 mA.

Under disturbances, our method can effectively determine the optimal beam orientation, as shown in Figure 5. The signal strength bounds at -39 dBm (upper) and -63 dBm (lower) in this case. In the four trials, the receiver's peak RSSI consistently reached approximately -39 dBm, while both the mean and median values converged near -45 dBm, demonstrating that the optimal beam was successfully maintained in a dynamic environment.

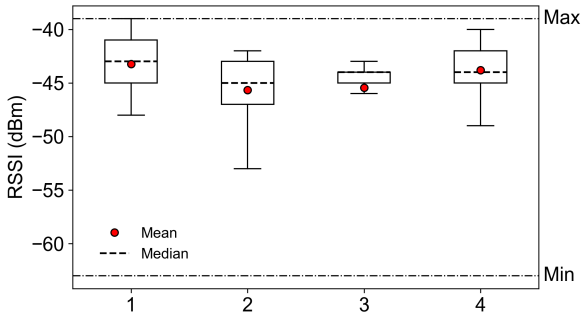

Fig. 5: RSSI results when aligned to the optimal beam after four complex disturbances. The RSSI upper limit is -39 dBm, and the lower limit is -63 dBm.

Conclusion and Future Work

In this study, we propose utilizing the IMUs in ingestible electronics and receivers to compute their attitude, provide feedback on the optimal beam direction, and align the receiver antenna accordingly to mitigate communication instability. Using the Mahony filter and visualizing in Blender, we estimated the attitudes of both the ingestible electronics and the receiver. We validated that Chip, Helical, PCB, and FPC each possess a directivity. We demonstrated that aligning the receiver with the optimal beam yields stable communication. Experimental results demonstrate that, by continuously tracking the ingestible electronics' optimal beam, a 4 dB gain is achieved, corresponding to a 32% reduction in maximum current consumption (TXP from 8 to 4 dBm). This performance is maintained under four complex motions. Future work should consider the attenuation of tissues, which may necessitate establishing a mapping between position and tissue-induced attenuation.

REFERENCES

[1] C. Steiger, A. Abramson, P. Nadeau, A. P. Chandrakasan, R. Langer, and G. Traverso, "Ingestible electronics for diagnostics and therapy," *Nature Reviews Materials*, vol. 4, pp. 83–98, feb 2019.

[2] P. A. Thwaites, C. K. Yao, E. P. Halmos, J. G. Muir, R. E. Burgell, K. J. Berean, K. Kalantar-Zadeh, and P. R. Gibson, "Review article: Current status and future directions of ingestible electronic devices in gastroenterology," *Alimentary Pharmacology & Therapeutics*, vol. 59, no. 4, pp. 459–474, 2024.

[3] A. Abdigazy, M. Arfan, G. Lazzi, C. Sideris, A. Abramson, and Y. Khan, "End-to-end design of ingestible electronics," *Nature Electronics*, vol. 7, pp. 102–118, Feb 2024.

[4] S. L. Cotton, R. D'Errico, and C. Oestges, "A review of radio channel models for body centric communications," *Radio Science*, vol. 49, no. 6, pp. 371–388, 2014.

[5] H. Chen and A. S. Lou, "A study of rf power attenuation in bio-tissues," *Journal of Medical and Biological Engineering*, vol. 24, pp. 141–146, 2004.

[6] A. Mauludiyanto, G. Hendrantoro, and M. Nova, "The attenuation characteristics of the body tissue on frequency function in wban channel," *JAREE (Journal on Advanced Research in Electrical Engineering)*, vol. 5, 10 2021.

[7] D. Sarma, A. O. Asok, and S. Dey, "Designing a meanderline-based ultraminiature low-profile ultrawideband antenna for biomedical applications," *2024 IEEE Wireless Antenna and Microwave Symposium (WAMS)*, pp. 1–5, 2024.

[8] X. Cheng, J. Wu, R. Blank, D. E. Senior, and Y.-K. Yoon, "An omnidirectional wrappable compact patch antenna for wireless endoscope applications," *IEEE Antennas and Wireless Propagation Letters*, vol. 11, pp. 1667–1670, 2012.

[9] X. Wang and X. He, "Research on attitude representations and attitude differential equations," in *Proceedings of the 2018 International Conference on Computer Modeling, Simulation and Algorithm (CMSA 2018)*, pp. 180–184, Atlantis Press, 2018/04.

[10] S. A. Ludwig and K. D. Burnham, "Comparison of euler estimate using extended kalman filter, madgwick and mahony on quadcopter flight data," in *2018 International Conference on Unmanned Aircraft Systems (ICUAS)*, pp. 1236–1241, 2018.

[11] M. Liu, Y. Cai, L. Zhang, and Y. Wang, "Attitude estimation algorithm of portable mobile robot based on complementary filter," *Micromachines*, vol. 12, no. 11, 2021.

[12] F. Farhangian and R. Landry, "Accuracy improvement of attitude determination systems using ekf-based error prediction filter and pi controller," *Sensors*, vol. 20, no. 14, 2020.

[13] Y. Jeon, S. Maji, S. Yang, M. S. S. Thaniana, A. Gierlach, I. Ballinger, G. Selsing, I. Moon, J. Jenkins, A. Pettinari, N. Fabian, A. Hayward, G. Traverso, and A. Chandrakasan, "Secure and stable wireless communication for an ingestible device," *2023 45th Annual International Conference of the IEEE Engineering in Medicine Biology Society (EMBC)*, pp. 1–6, 2023.

[14] C. Liu, Y. xin Guo, and S. Xiao, "Circularly polarized helical antenna for ism-band ingestible capsule endoscope systems," *IEEE Transactions on Antennas and Propagation*, vol. 62, pp. 6027–6039, 2014.

[15] W. Seo, U. Kim, S. Lee, K. Kwon, and J. Choi, "A meandered inverted-f capsule antenna for an ingestible medical communication system," *Microwave and Optical Technology Letters*, vol. 54, 2012.

[16] G. Traverso, J. Finomore, Victor, I. Mahoney, James, J. Kupec, R. Stansbury, D. Bacher, B. Pless, S. Schuetz, A. Hayward, R. Langer, and A. Rezai, "First-in-human trial of an ingestible vitals-monitoring pill," *Device*, vol. 1, nov 2023.

[17] P. Poshtgol, S. Soltani, and R. Murch, "Printed high gain end-fire beam-steerable yagi antenna," *2017 IEEE International Symposium on Antennas and Propagation USNC/URSI National Radio Science Meeting*, pp. 163–164, 2017.